JOURNAL OF GUIDANCE, CONTROL, AND DYNAMICS
Vol. 27, No. 4, July–August 2004

Tuning of Observer-Based Controllers

C. Cumer* and F. Delmond†
ONERA–Centre d'Etudes et de Recherches de Toulouse, 31055 Toulouse, France
and
D. Alazard‡ and C. Chiappa§
SUPAERO, 31055 Toulouse, France

A particular postsynthesis problem is examined. Assume a first complex controller running on a given system. It turns out that a closed-loop mode is not sufficiently damped. Is it easy to know which adjustable combinations of controller parameters are the most relevant to master this problem? A Bayesian identification procedure is proposed to analyze the relevance of such a given parameter combination with respect to a given modal specification. One application, for which such a controller tuning is very interesting, is the adjustment of flight control laws during flight tests. In this practical context, the observer-based realization of the controller is used to derive an architecture suitable for its implementation, that is, an architecture in which physical tuning parameters can be easily highlighted. The results presented concern the lateral flight control law of a highly flexible aircraft that has been synthesized by a modern robust control approach.

Nomenclature

$\left[\begin{array}{c\|c} A_l & B_l \\ \hline C_l & D_l \end{array}\right]$	=	state-space realization of model $G_l(s)$
A^T	=	transposed of matrix A
dp	=	aileron deflection, deg
dr	=	rudder deflection, deg
$G(s)$	=	synthesis model
$G_f(s)$	=	full-order model (validation model)
$G_o(s)$	=	onboard model
$G_r(s)$	=	fourth-order rigid model
$K(s)$	=	nominal dynamic output feedback
K_{c_r}	=	rigid part of the onboard state feedback
K_{x_r}	=	rigid state feedback
n_{y_i}	=	lateral acceleration at measurement point number i, (m/s^2)
p	=	roll rate, deg/s
p_{ref}	=	pilot input, roll
q_j	=	generalized coordinate of flexible mode number j
r	=	yaw rate, deg/s
s	=	Laplace variable
spec(A)	=	eigenvalues of a square matrix A
$\boldsymbol{u}$	=	control input vector, $[dp \;\; dr]^T$
$\dot{x}$	=	time derivation, $\partial x/\partial t$
$\boldsymbol{x}_r$	=	rigid state vector, $[\beta \;\; p \;\; r \;\; \phi]^T$
β	=	yaw angle, deg
β_{ref}	=	pilot input, yaw
ϕ	=	roll angle, deg

Presented as Paper 2001-4102 at the Guidance, Navigation and Control Conference, Montreal, CA, 6 August 2001; received 16 July 2003; revision received 10 October 2003; accepted for publication 13 October 2003.

*Research Engineer, Department of System Control and Flight Dynamics; cumer@cert.fr.
†Ph.D. Student, Department of System Control and Flight Dynamics.
‡Professor, Automatic Control Department.
§Professor, Automatic Control Department; also Research Engineer, Department of System Control and Flight Dynamics, ONERA, 31055 Toulouse, France.

Introduction

THE transfer of modern control techniques from the research world to the industrial world often encounters implementation problems, both from the controller order point of view and from the architecture of this controller. Industrial solutions to solve control problems are often based on important know-how and consist of a set of static gains completed with judicious filters, integrators, saturations, etc. The gains and the states of such a controller have physical units, and knowledge of the controller is very useful to perform last-minute tunings.

On the other hand, flexible structures (aircrafts, satellites, launchers, etc.) raise many control problems. These are particularly relevant with applications to evaluate control law synthesis techniques, and classical approaches can fail on such problems. Thus, during the last decade, much literature concerning the application of robust control design techniques to flexible structures[1–6] has become available. However, these approaches are often based on optimal control [H_∞, H_2, Linear Quadratic Gaussian synthesis, μ-synthesis] and produce high-order controllers expressed under a meaningless state-space realization. These last points are particularly relevant if a controller reduction has been performed. Then it is nearly impossible to adjust control tuning parameters if the synthesis model or specifications should be changed.

The main problem raised in this paper is the adjustment of a given control law to achieve new specified closed-loop dynamics properties. The goal is to find a suitable combination of controller parameters, called the tuning direction, that is able to master this modal specification. The scalar gain along this tuning direction is called the potentiometer. Its value is not really of interest because it will be adjusted in situ on the real system. However, to analyze such a tuning direction, we need a validation model, that is, the most representative model, whose order is generally greater than the compensator order. Moreover, some controller structures allow a relevant tuning direction to be easily highlighted. However, it is not the general case, as explained before. It is clear that, if the controller states are physical, the industrial know-how can directly give possible tuning directions.

The first subproblem of how a given controller can be interpreted from a physical point of view is not well addressed in the literature. Recently, one can find some contributions on similar implementation problems. Among others, in Ref. 7 the author proposes new controller architecture to handle fault tolerant control problems in a two steps design procedure: a first pure-performance synthesis and then a second synthesis based on the Youla parameterization. The Youla parameterization can also be used to compute an equivalent observer-based structure of a given controller (see Ref. 8).

Interest of such a structure lies in that the controller states become meaningful variables, that is, an estimate of the plant states. Then, one can express all of the gains and all of the states of the controller with a physical unit if the plant states are physical variables. Moreover, physical considerations can guide the selection of tuning directions to adjust some closed-loop modal characteristics. This paper also exploits this result, but the main idea is to use a judiciously selected onboard model to develop the onboard observer-based structure. This onboard model must be a physical model restricted to the main dynamic behavior we want to master by direct potentiometers.

Once these tuning directions have been identified, the second subproblem of how the tuning directions can be judged as good or bad for achieving a new modal specification on closed-loop validation model is a postsynthesis challenge rarely studied. In other words, it is an analysis phase that quantifies the relevance of these tuning directions. We propose here to use the parameter robust analysis by Bayesian identification (PRABI) tool.[9–11] This theoretical parametric robust analysis tool is here extended to a tuning direction analysis tool.

A particular application is the implementation and adjustment of flight control laws during aircraft flight tests.[12,13] Alazard[13] constructed an onboard model and an observer-based controller architecture and highlighted high-level tuning parameters based on physical considerations and good sense rules to improve flying qualities. In this paper, the PRABI mathematically quantifies the relevance of these intuitive tuning directions.

The paper is outlined as follows. First the controller structure used to identify physically tuning directions is described. The subtle difference between the onboard model and the validation model is clarified. It is shown that, if the order of the controller is greater than or equal to the order of the plant, that is, if one can choose the validation model as the onboard model, the modal control theory can be used to derive perfect tuning direction to master any closed-loop modal specification. The PRABI and its adaptation to the modal tuning problem in the general case, where the validation model order is greater than the controller order, is presented. The key idea is to determine if a fictive variation of a closed-loop modal characteristic (damping ratio, pulsation) can be counterbalanced by a potentiometer value. In an identification framework, this result defines a direction of insensitivity. Finally, the tuning method is successfully applied to a lateral flight control law of a highly flexible aircraft,[12,13] and a numerical analysis of different tuning directions is made.

Observer-Based Structure Used for Physical Tuning

Validation/Onboard Models

Mathematical modeling of the physical dynamics is one of the primary considerations in control system design. For large mechanical systems, this step often requires a finite element computation. Consequently, models are high ordered.

As modern control techniques are applied, controllers have at least the same order as the model. Then the implementation of such controllers could raise many problems. To overcome these problems, there are two ways to produce reduced-order controllers.

1) The model itself is reduced before the control synthesis step; the complete model is called the validation model, whereas the reduced model is designated as the synthesis model.

2) The controller can be reduced after the synthesis. One can reconstruct a model that can be used to implement the reduced controller as an observer-based controller (using the procedure presented in Ref. 8). Such a model is referred as an onboard model.

Advantages of the Observer-Based Controller Structure

As already mentioned, the search of tuning directions is only performed with an onboard observer-based realization of the control law. Three reasons explain this choice.

1) This control structure, represented in Fig. 1 is not restrictive. (In Fig. 1, direct feedthrough is ignored for clarity.) The parameters K_c (state feedback gain), K_f (state estimator gain), and $Q(s)$ (dynamic Youla parameter), which entirely define a general observer-based

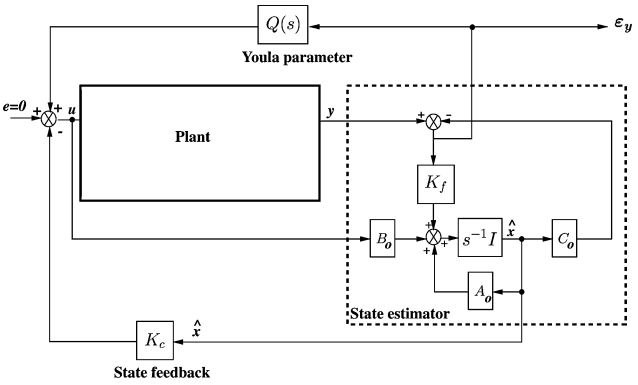

Fig. 1 Youla parameterization with observer-based structure.

structure, can be computed to be exactly equivalent with the original controller.[8,13] Note that there are several solutions, which depend on the choice of the distribution of the closed-loop eigenvalues between the state-space dynamics [spec$(A_0 - B_0K_c)$], the state-estimation dynamics [spec$(A_0 - K_fC_0)$], and the Youla parameter dynamics [spec (A_Q)], where A_Q, B_Q, C_Q, and D_Q indicate the Youla parameter state-space realization. Some remarks in Ref. 8 aided in the construction of an equivalent observer-based controller.

2) Moreover, a state-space representation of an observer-based controller can be interpreted as plant state estimate. This physical interpretation allows the most important physical gains to be extracted quickly from the control law.

3) The observer-based realization has a minimal number of significant parameters.

Controller Adjustment Using Modal Theory

Let us suppose the modal characteristics (pulsation, damping ratio) of the plant are changing and we want to adjust the controller to master the closed-loop dynamics. If the controller order is greater or equal to the validation model order, the onboard model can be chosen as the validation model (A_0, B_0, C_0, and D_0 in Fig. 1). Then all of the closed-loop eigenvalues are included in spec$(A_0 - B_0K_c)$ and spec$(A_0 - K_fC_0)$. Whatever the new specification on a closed-loop eigenvalue, one can find a new state-feedback gain K_c (or the new state-estimation gain K_f) by use of eigenstructure assignment theory that will fulfill the new specification. Therefore, tuning directions can be easily highlighted. That is explained in the sequel.

Notations for Standard Eigenvector Assignment

Let consider the following linear system with n states, m inputs, and p outputs:

$$\dot{\boldsymbol{x}} = A_0\boldsymbol{x} + B_0\boldsymbol{u}, \qquad \boldsymbol{y} = C_0\boldsymbol{x} + D_0\boldsymbol{u} \tag{1}$$

where $\boldsymbol{x}$ is the state vector, $\boldsymbol{y}$ the vector of measurements, and $\boldsymbol{u}$ the input vector. Consider a state feedback $K \in \mathbb{R}^{m\times p}$: $\boldsymbol{u} = K\boldsymbol{x}$. The closed-loop state matrix is

$$A_{\text{cl}} = A_0 + B_0K$$

The following notation is often used: λ_i and $\boldsymbol{u}_i$ are, respectively, the ith closed-loop eigenvalue and its corresponding right eigenvector, and $w_i = K\boldsymbol{u}_i$. The classical closed-loop eigenvalue assignment procedure assigns n dynamics with the solution,[14,15]

$$K = [w_1 \quad \cdots \quad w_p][\boldsymbol{u}_1 \quad \cdots \quad \boldsymbol{u}_p]^{-1}$$

where

$$[A_0 - \lambda_i I \quad B_0]\begin{bmatrix}\boldsymbol{u}_i\\ w_i\end{bmatrix} = 0 \tag{2}$$

Postsynthesis Tuning of a Closed-Loop Eigenvalue Damping

Consider a flexible system and suppose that an observer-based controller is first obtained. Let K_c denote the state-feedback gain issued from this control law. It turns out that a flexible mode is not sufficiently damped. The standard pole placement synthesis easily gives a state-feedback gain K_{c1} that only changes the flexible mode damping in closed-loop dynamics [see Eq. (2)]. The difference $dK_c = K_c - K_{c1}$ clearly defines a local direction for the expected damping variation. Given a scalar λ, then λdK_c locally tunes the desired flexible mode damping. In other words, λ is the potentiometer to be tuned along the tuning direction dK_c.

This modal tuning method based on the onboard model is very fast and presents good readability. A mathematical expression for tuning directions is easily obtained. Moreover, this method is attractive because additional constraints on closed-loop eigenvectors can be set. For example, decoupling constraints only implies that Eq. (2) is replaced by

$$\begin{bmatrix} A_0 - \lambda_i I & B_0 \\ E_i & F_i \end{bmatrix} \begin{bmatrix} \boldsymbol{u}_i \\ w_i \end{bmatrix} = 0$$

in which the matrices $E_i \in \mathbb{R}^{(m-1)\times n}$ and $F_i \in \mathbb{R}^{(m-1)\times m}$ describe the expected decoupling properties.

However, its principal drawback is that it does not work if the validation model order is greater than the controller order. This case often occurs in the field of flexible structures. Indeed, the extracted potentiometers are not systematically relevant to the validation model because the separation principle is no longer verified. Moreover, no guarantee of stability and performance of the tuned validation model is assured here.

That is the reason why it is necessary to have a tool that can quantify the tuning direction relevance according to the tuning objective on the validation model. The next section proposes an heuristic, the PRABI, initially conceived for parametric robust analysis and applied here to the tuning framework.

Analysis of Tuning Directions via PRABI Method

Basic Notions of PRABI

The PRABI robust analysis method is based on a measure of the identifiability of closed-loop system parameters.

Indeed, the covariance matrix G_Θ of the steady-state parametric estimation error is computed as if a Bayesian identification of some system parameters $\boldsymbol{\Theta}$ had been performed. Let $\boldsymbol{\Theta}_0$ denote the nominal parametric vector. The probability that the parametric vector $\boldsymbol{\Theta}$ is identified far from $\boldsymbol{\Theta}_0$ with a quantity equal to $\Delta\boldsymbol{\Theta}$ follows a Gaussian law as

$$p(\boldsymbol{\Theta}_0 + \boldsymbol{\Delta\Theta}) = \Lambda \exp\left(-\boldsymbol{\Delta\Theta}^T G_{\Theta_0}^{-1} \boldsymbol{\Delta\Theta}\right) \tag{3}$$

where Λ is a constant and $G_{\Theta_0}^{-1}$ the inverse of the covariance matrix. (The calculation of $G_{\Theta_0}^{-1}$ may be found in Refs. 9, 10, and 11.)

What is most important is the interpretation of the result: the harder a parametric combination is to identify, the less sensitive is the closed-loop system is toward this combination and vice versa.

Better still, let us consider the ith unitary eigenvector $\Delta\boldsymbol{\Theta}_i$, related to the ith eigenvalue λ_i of $G_{\Theta_0}^{-1}$. In this parametric direction, the density of probability has the following profile:

$$p(\boldsymbol{\Theta}_0 + \alpha\Delta\boldsymbol{\Theta}_i) = \Lambda \exp\left(-\lambda_i \alpha^2\right) \tag{4}$$

Consequently, the eigenvectors related to the minor and major eigenvalues of $G_{\Theta_0}^{-1}$ correspond, respectively, to the minimal and maximal system sensitivity directions in the parametric space.

Notice that this parametric sensitivity analysis is a local study. When used, this tool necessarily implies iterative algorithms. In the context of parametric robust analysis, the basic idea is that the less robust a closed-loop system is to a parametric variation, the more sensitive this system is toward this modification. The moving along successive maximal sensitivity directions also gives the nearest parametric worst case.[9] The next section is devoted to the PRABI extension to the tuning direction relevance analysis.

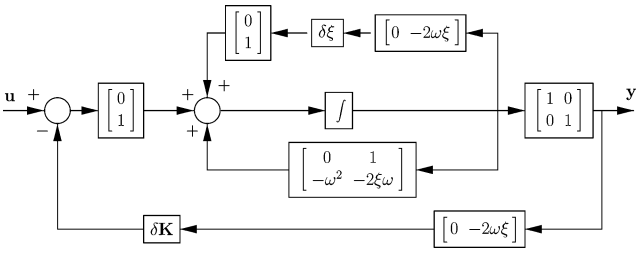

Fig. 2 Potentiometer for a damping variation on a simple system.

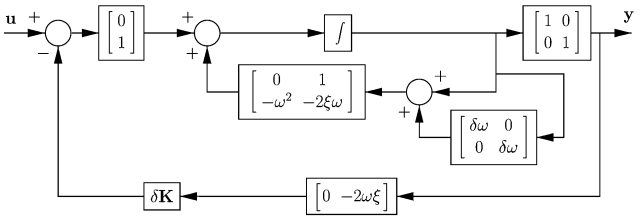

Fig. 3 Potentiometer for a pulsation variation on a simple system.

Use of the PRABI Method for Tuning Direction Analysis

To analyze the relevance of a potentiometer, the parametric vector is composed of 1) the scalar potentiometer, introduced in the controller structure, to fulfill the tuning objective and 2) the fictive modal characteristic variation, a scalar, like a damping variation $\delta\xi$, on which the tuning direction should to be focused.

If the potentiometer only affects this modal characteristic, that is, the modal variation can be exactly countered by the potentiometer value along the tuning direction, a direction of insensitivity must appear, and the matrix $G_{\Theta_0}^{-1}$ loses a rank. (The $G_{\Theta_0}^{-1}$ minor eigenvalue then equals zero.)

A simple example given in Fig. 2 shows this loss of rank. A relative damping variation of a second-order open-loop system is modeled with the $\delta\xi$ parameter. Clearly, the tuning direction δK is used to counterbalance exactly this variation. In other words, here δK is a perfect tuning direction to master the damping variation.

The PRABI tool detects this tuning direction accuracy. If $[\delta\xi \;\; \delta K]^T$ describes the parametric vector variation $\Delta\boldsymbol{\Theta}$, then $G_{\Theta_0}^{-1}$ is always equal to

$$G_{\Theta_0}^{-1} = \begin{bmatrix} 0.0323 & -0.0323 \\ -0.0323 & 0.0323 \end{bmatrix}$$

when the initial values of ω and ξ are 3rd/s and 0.5, respectively. Its two eigenvalues are 0 (whatever the initial values of ω and ξ) and 0.0646. The nullity of its minor eigenvalue proves that the system is completely insensitive to a parametric direction. This particular direction is defined by the eigenvector related to the minor eigenvalue. (Here $\delta K - \delta\xi = 0$.) When the fictive variation $\delta\xi$ disappears, the tuning direction will do exactly the opposite of this variation.

Now, if the variable parameter is the pulsation (Fig. 3), the same tuning direction δK is no longer relevant to counterbalance this relative variation $\delta\omega$. Similar computations yield the following numerical value for $G_{\Theta_0}^{-1}$:

$$G_{\Theta_0}^{-1} = \begin{bmatrix} 0.1353 & 0.0284 \\ 0.0284 & 0.0323 \end{bmatrix}$$

No loss of matrix rank is observed because the eigenvalues of $G_{\Theta_0}^{-1}$ are 0.025 and 0.1426, respectively. In other words, no parametric direction of complete insensitivity is detected. In this case, the tuning direction is not really adequate for this new tuning objective.

These two applications show that the condition number of $G_{\Theta_0}^{-1}$ quantifies the quality of a potentiometer relevance. In the first case, this number is infinite, whereas it only equals 5.7 in the second case. Of course, these condition numbers can give a tuning direction relevance comparison only if evaluated on the same system.

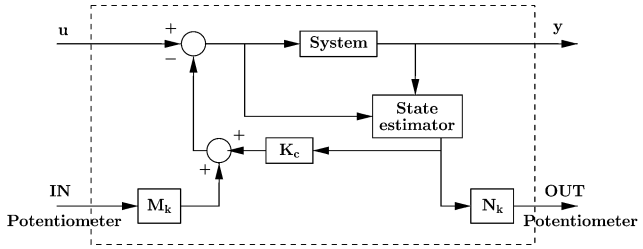

Fig. 4 Potentiometer extraction.

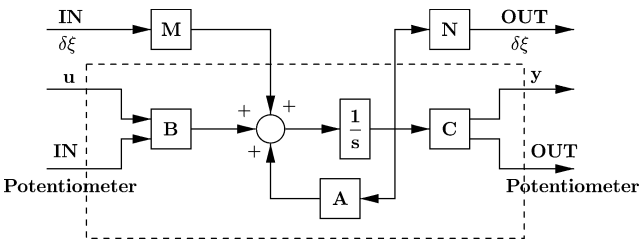

Fig. 5 Parameter extraction.

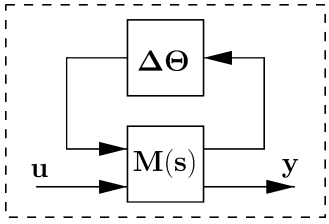

Fig. 6 Standard form of the PRABI analysis problem.

Standard Form for Modal Specification Tuning on Closed-Loop System

The preceding example deals with open-loop modal characteristics. As shown in Fig. 2, the fictive modal variation can be easily highlighted from the system by the introduction of fictive inputs and outputs. This kind of modeling, often called standard form $M-\Delta$ modeling or linear fractional transformation modeling in a robustness framework, is not indispensable to the tuning problem, but does have the advantage of being practical and readable.

The problem here is similar, but it concerns the quantification of controller gains combinations (tuning directions) relevance for a modal closed-loop modification. This problem is more difficult to put into the corresponding standard form.

The first step consists in highlighting the potentiometer and its tuning direction from the control law. When the controller is observer based, the state feedback matrix K_c contains the most adapted gains to a modal tuning. Each gain can be tuned differently; the matrices M_k and N_k (as in Fig. 4) manage by the variation of all gains independently. Then, the increased system inside the dotted line (Fig. 4) is represented in its state-space block diagonal realization, where a block relative to two complex conjugate eigenvalues reads

$$\begin{bmatrix} 0 & 1 \\ -\omega_i^2 & -2\xi_i\omega_i \end{bmatrix}$$

where increased system means that the number of inputs and outputs has increased. Similarly to the modelization explained in the preceding section, matrices M and N are introduced to take into account the variation of closed-loop dynamics (as shown in Fig. 5 for a damping variation).

The final standard form $M-\Delta$ (Fig. 6) puts together closed-loop dynamics variation and potentiometer into the $\Delta\Theta$ block.

Application to Flexible Aircraft Flight Control

Model and Specifications

This section summarizes the model, the specifications, and the robust design procedure presented in a previous paper.[12] The model used for this study is a linearized model of the lateral motion of a flexible aircraft around an equilibrium point. The system is a large carrier aircraft in which flexibility was intentionally degraded to evaluate the relevance of control law synthesis techniques on a very critical case. The model is a 60th-order state-space representation with 2 control inputs (aileron deflection dp and rudder deflection dr) and 44 measurements, 4 measurements (lateral acceleration n_{y_i}, roll rate p_i, yaw rate r_i, and roll angle ϕ_i) in 11 measurement points regularly spaced along the fuselage, $i=1,\ldots,11$. The state vector $\boldsymbol{x}$ contains 4 rigid states (yaw angle β, roll rate p, yaw rate r, and roll angle ϕ); 36 states that represent the 18 flexible modes modelled between 8 and 80 rd/s (generalized coordinates q_j and $\dot{q}_j$, $j=1,\ldots,18$); and 20 secondary states that represent dynamics of servocontrol surfaces and aerodynamic lags.

The full-order model on which controllers will be validated in the following is noted $G_f(s)$. We will also refer to the corresponding rigid model $G_r(s)$, in which only the 4 rigid states $(x_r=[\beta, p, r, \phi]^T)$ are considered, and the 30th-order synthesis model $G(s)$. The reduction procedure to obtain this synthesis model from the full-order model G_f is detailed in Ref. 12.

The following list summarizes the various specifications: S1, Dutch roll damping ratio >0.5; S2, templates on the step responses with respect to β and p; S3, roll/yaw channel decoupling; S4, no degradation of the damping ratios of flexible modes, or furthermore, an increase of the damping ratios of low-frequency flexible modes to improve comfort during turbulence; S5, previous performances must be robust with respect to the various cases of loading; and S6, to use a reasonable number of measurements (between 4 and 10).

Modal and time-domain specifications S1–S3 concern the rigid dynamics of the aircraft. If the system is assumed to be rigid, eigenstructure assignment techniques are particularly effective to handle these specifications, especially because we have a number of outputs ($\geq$4) sufficient to implement an ideal rigid state feedback by a static output feedback. These techniques will not be detailed in this paper.[16] A rigid state feedback K_{x_r} on the four rigid states $\boldsymbol{x}_r$ was, thus, calculated on model G_r to meet the following modal specifications (as in Chap. 8, Part. 3 in Ref. 17):

1) The Dutch roll mode is assigned to $-1+1.3\,i$ and is decoupled from ϕ.

2) The pure roll mode is assigned to -1.1 and is decoupled from β.

3) The spiral mode is assigned to -1 and is decoupled from β.

Time responses obtained on the rigid model G_r are presented in Fig. 7 (black curves). These responses satisfy S1–S3 and will be used as a reference to judge the solutions proposed on the full-order model G_f. This simulation plots the rigid state responses $[\beta(t), \phi(t)\ p(t)$, and $r(t)]$ to β_{ref} and p_{ref} step inputs. In fact, the real command that is applied reads

$$\begin{bmatrix} dp \\ dr \end{bmatrix} = H \begin{bmatrix} \beta_{\text{ref}} \\ \dfrac{1}{s}\, p_{\text{ref}} \end{bmatrix} - K_{x_r}\, x_r \tag{5}$$

where H is a feedforward static matrix computed to ensure the steady-state constraint,

$$\lim_{t\to\infty} \begin{bmatrix} \beta(t) \\ \phi(t) \end{bmatrix} = \begin{bmatrix} 1 & 0 \\ -1 & 1 \end{bmatrix} \begin{bmatrix} \beta_{\text{ref}} \\ \dfrac{1}{s}\, p_{\text{ref}} \end{bmatrix} \tag{6}$$

Thus, the problem can be now restated in the following way: To synthesize a control law satisfying the frequency domain and modal specifications S4 on the flexible modes and to preserve as much as possible the performances on the rigid modes obtained with the modal gain K_{x_r}, the whole process has to be made under the robustness requirement S5 and the hardware constraint S6.

To evaluate the various syntheses, we will also analyze the root locus of the loop transfer $L(s)=-K(s)G_f(s)$ obtained while varying feedback gains from 0 to 1 simultaneously on both control channels dp and dr. (Positive feedback is assumed for dynamic output feedback.) (See Fig. 8 as an example: $\times$ and $+$ indicate open-loop

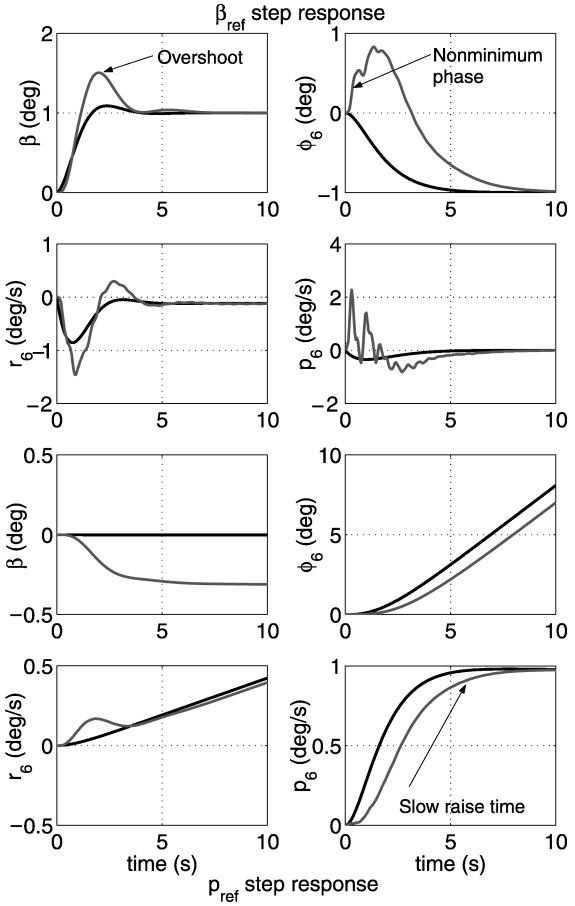

Fig. 7 Simulations: black, nominal rigid [K_{x_r} with $G_r(s)$] and gray, nominal full [$K(s)$ with $G_f(s)$].

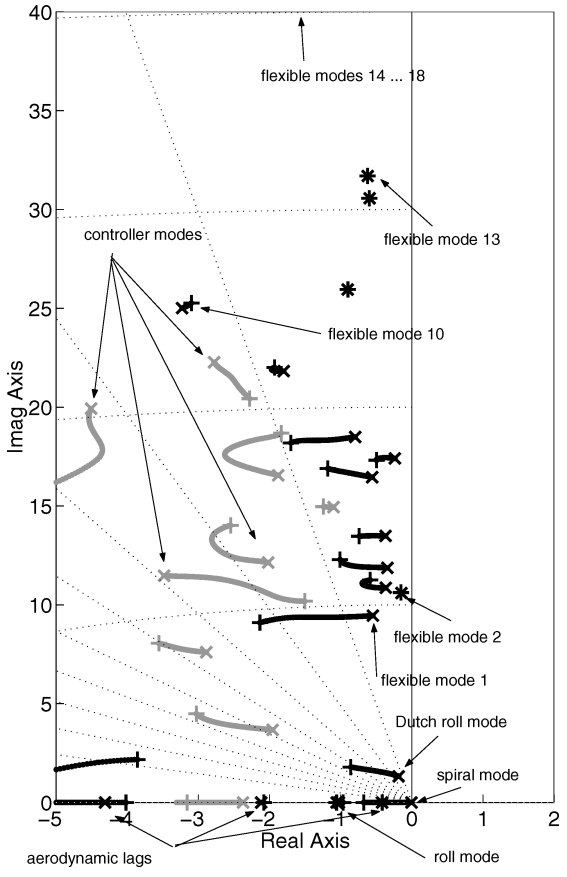

Fig. 8 $-K(s)G_f(s)$: root locus.

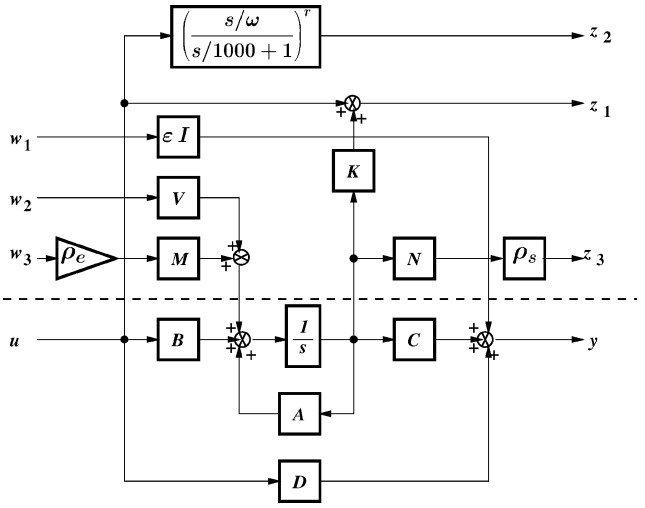

Fig. 9 Setup for active synthesis.

and closed-loop poles, respectively, and gray trajectories correspond to controller poles).

The control design procedure is a robust H_2 synthesis on the standard problem shown in Fig. 9. However the controller is performed, the tuning procedure is the same. That is the reason why the synthesis procedure is not precised. (For more information, see Refs. 12 and 13.)

This H_2 synthesis provides a 36th-order controller ($30 + 2 \times 3$ because the nominal tuning is $r = 3$), which has been reduced to the 20th order by a direct balanced reduction and denoted $K(s)$. Then the nominal root locus and time-domain simulation [on the full-order model $G_f(s)$] are displayed in Figs. 8 and 7 (gray curves), respectively. Note that flexible mode damping ratios are increased in closed loop. On the other hand, time responses are not adequate with respect to the pure rigid behavior: The overshoot on β, the nonminimum phase response on ϕ for a step in β_{ref}, and the too slow rise time on p must be improved.

Onboard Model and Onboard Controller Architecture

Once the controller has been reduced, its state-space realization does not present any particular structure and cannot be interpreted as a plant state estimate. Here, we are going to express this controller as an observer-based controller built on a judiciously selected onboard model $G_o(s)$ (A_o, B_o, C_o, D_o) according to Fig. 1.

In this application, we have chosen a 20th onboard model, that is, the same order as the controller order. (This choice will lead to a static Youla parameter.) This model is only representative of the main modes on which the control has an effective action, that is, the rigid modes (4 states, $x_r = [\beta, p, r, \phi]^T$) and the flexible modes number 1 and 3–9 (for a total of 16 states). One can verify on nominal root locus (Fig. 8) that, although flexible modes 10–13 are taken into account in the synthesis, the control law has no influence on them.

This onboard model is represented with a block diagonal realization associated with the state vector:

$$\boldsymbol{x}_o = \left[\boldsymbol{x}_r^T, \ldots, q_j, \dot{q}_j, \ldots\right]^T, \qquad j = 1, 3, 4, \ldots, 9 \tag{7}$$

and this realization is

$$\left[\begin{array}{cccccc|c} A_r & 0 & \ldots & \ldots & \ldots & 0 & B_r \\ 0 & A_1 & \ddots & & & \vdots & B_1 \\ \vdots & \ddots & \ddots & \ddots & & \vdots & \vdots \\ \vdots & & \ddots & A_j & \ddots & \vdots & B_j \\ \vdots & & & \ddots & \ddots & 0 & \vdots \\ 0 & \ldots & \ldots & \ldots & 0 & A_9 & B_9 \\ \hline C_r & C_1 & \ldots & C_j & \ldots & C_9 & D_{o_{6\times 2}} \end{array}\right] \tag{8}$$

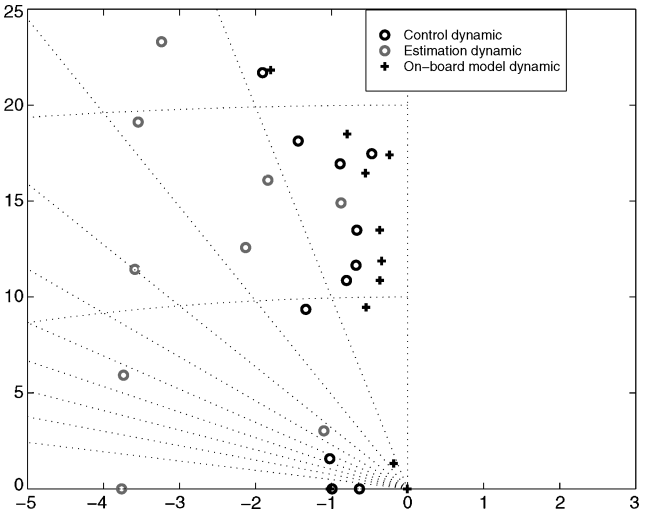

Fig. 10 Eigenvalue distribution (around imaginary axis).

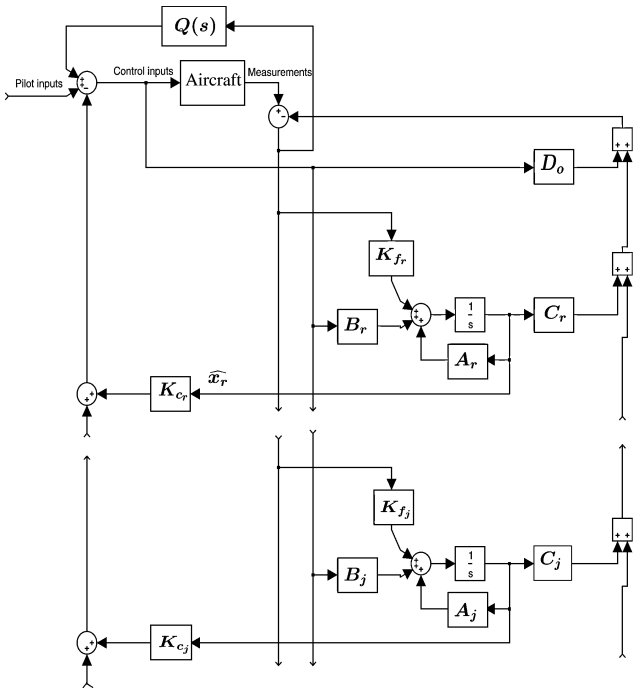

Fig. 11 Onboard controller parallel structure.

with $j = [1, 3, 4, 5, 6, 7, 8, 9]$ and, for the flexible eigenvalue λ_j,

$$A_j = \begin{bmatrix} \mathrm{Re}(\lambda_j) & -\mathrm{Im}(\lambda_j) \\ \mathrm{Im}(\lambda_j) & \mathrm{Re}(\lambda_j) \end{bmatrix} \tag{9}$$

The closed-loop eigenvalues distribution we have chosen is shown in Fig. 10: Among the 40 closed-loop eigenvalues, we have affected to state feedback dynamic $[\mathrm{spec}(A_o - B_o K_c)]$ the 20 eigenvalues that are the closest with the 20 onboard model eigenvalues.

The equivalent observer-based form built on such a model can be implemented according to the parallel structure shown in Fig. 11, where the state feedback gain K_c and the state estimation gain K_f have been partitioned according to the onboard model structure:

$$K_c = \left[K_{c_r}, \ldots, K_{c_j}, \ldots\right], \qquad K_f = \left[K_{f_r}^T, \ldots, K_{f_j}^T, \ldots\right]^T$$

Highlighting Tuning Directions

The tuning gains are purely and simply the main components of the state feedback gain K_c, that is, K_{c_r} to adjust the closed-loop rigid

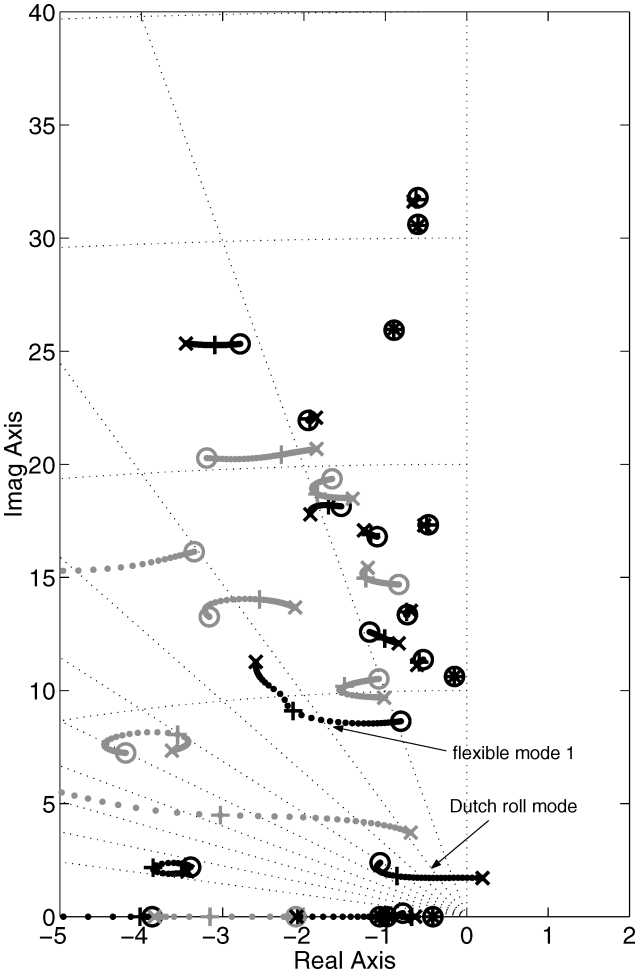

Fig. 12 Root locus around $K_{c_r}(2,3)$.

behavior and K_{c_j} to adjust the closed-loop flexible mode (number j) damping ratio.

Four adjustments have been performed on these potentiometers. The first three potentiometers have been quantified with the PRABI method. We will be able to compare the $G_{\Theta_0}^{-1}$ condition number with the results on root locus around these potentiometers and with the temporal responses.

Adjustment 1

Adjustment 1 is shown in Figs. 12 and 13. The purpose of this test is to act directly on the Dutch roll damping ratio. Physically, this can be performed by adjusting the gain between the yaw rate r and the rudder deflection d_r, that is, the second row, third column component of gain K_{c_r}: $K_{c_r}(2, 3)$. Note on the time-domain responses that this parameter (with a factor 0.5 or 2) acts directly on the Dutch roll because the response in β is governed by this mode (Fig 13). The roll axis response is insensitive to this tuning potentiometer. On the root locus (Fig. 12), also note that this potentiometer acts mainly on the Dutch roll mode and has a weak action on the flexible modes (where stability and damping are preserved) except for flexible mode 1. This flexible mode reveals a strong dynamic coupling with a nearby controller mode. In a more general way, controller dynamics is sensitive to this potentiometer.

Adjustment 2

Adjustment 2 is shown in Figs. 14 and 15. Here, the purpose is to accelerate the roll axis response (p step response) by a stronger control of the spiral mode: This can be performed by increasing the gain between the roll angle ϕ and the ailerons deflection d_p, that is, $K_{c_r}(1, 4)$. Like in the preceding case, this tuning does not affect the other modes, and the settling time on p is increased in a significant

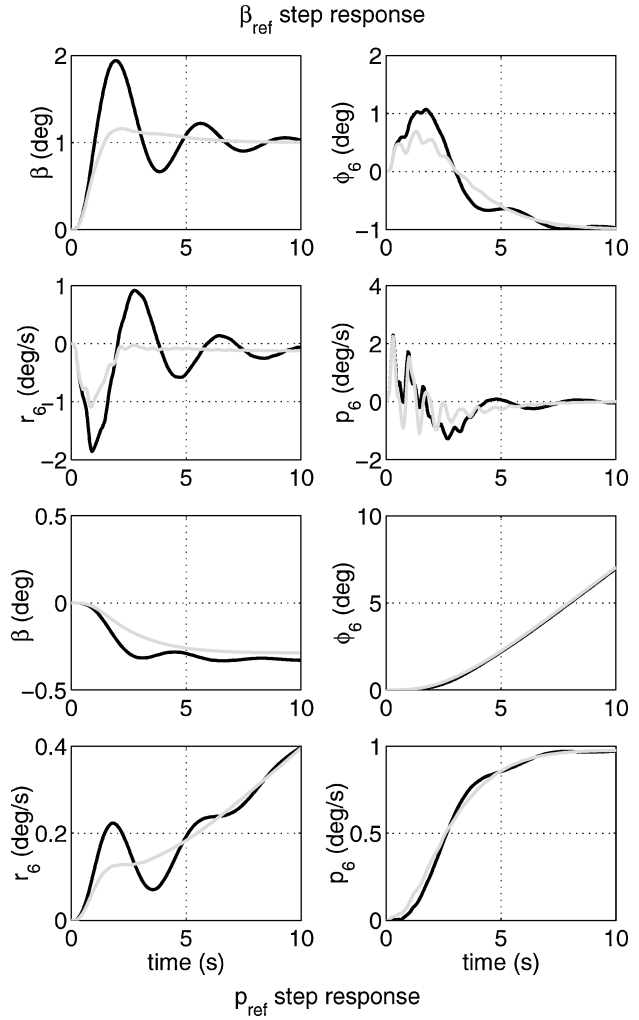

Fig. 13 Simulations: black, $K_{c_r}(2,3) = 0.5K_{c_r}(2,3)$ and gray, $K_{c_r}(2,3) = 2K_{c_r}(2,3)$.

way. The root locus (Fig. 14) is particularly demonstrative: This potentiometer works mainly on roll dynamics, whereas yaw dynamics (Dutch roll mode) and flexible dynamics are not very sensitive to this tuning.

Adjustment 3

Adjustment 3 is shown in Fig. 16. Here, the purpose is to act directly and only on the first flexible mode damping ratio. Figure 16 highlights that the variation of the gain K_{c_1} enables this damping ratio to be mastered, whereas the other flexible modes and the rigid dynamics are insensitive. Also note strong dynamic couplings with the controller modes and with a secondary plant mode (aerodynamic lag); the tuning range is, therefore, limited by these dynamic couplings.

Adjustment 4

Adjustment 4 is shown in Fig. 17. To avoid the nonminimum phase response, the rigid gain matrix K_{c_r} has been replaced with the modal rigid gain K_{x_r} computed on the pure rigid model. One can see that the time response (Fig. 17) is now similar to the nominal rigid response, whereas the flexible modes are always stabilized. This test confirms that the rigid state estimate $\widehat{x_r}$ highlighted in the new controller structure is effective.

Quantification of Potentiometer Relevance

To confirm the efficiency of the three physical potentiometers of the three first adjustments, parametric variation vector $\Delta\Theta$ must be constructed for each adjustment. For example, the first adjustment

Table 1 PRABI results

	$G_{\Theta_0}^{-1}$	
Potentiometer extracted for	Minor eigenvalue	Condition number
Dutch roll	4.7310^{-4}	4
Spiral	210^{-4}	93
First flexible mode	1.2510^{-3}	12

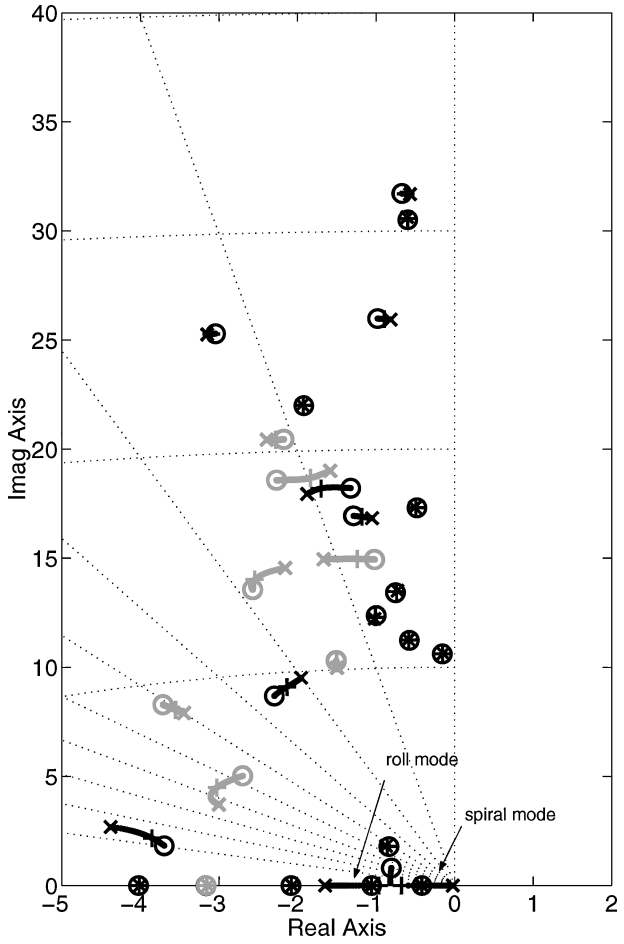

Fig. 14 Root locus around $K_{c_r}(1,4)$.

is characterized by

$$\Delta\Theta = \left[\delta\xi_{\text{Dutch roll}} \quad \delta K_{C_r}(2,3)\right]^T$$

Table 1 summarizes the condition index and the minor eigenvalue of the $G_{\Theta_0}^{-1}$ matrix obtained at each tuning case.

Even if the condition number represents the tuning direction efficiency on the fictive closed-loop characteristic, this quantity is not sufficient. Indeed, the minor eigenvalue gives further information. The higher the minor eigenvalue is, the less selective the tuning direction is. The displacements of the other poles are no more negligible.

These results show that the spiral mode potentiometer is the most efficient. Indeed, the high condition index of the respective matrix $G_{\Theta_0}^{-1}$ proves that the potentiometer correctly acts on spiral mode, and in addition, the low value of its minor eigenvalue indicates that the potentiometer does not perturb the other modes of the system (Fig. 14). Note that the fictive identification is led through the observation matrix C_f. The PRABI cannot detect the displacement of the weakly identifiable modes. This has no importance here because these mode are barely observable by the system outputs.

Similarly, the potentiometer dedicated to the first flexible mode tuning is more revelant than the one extracted for the Dutch roll

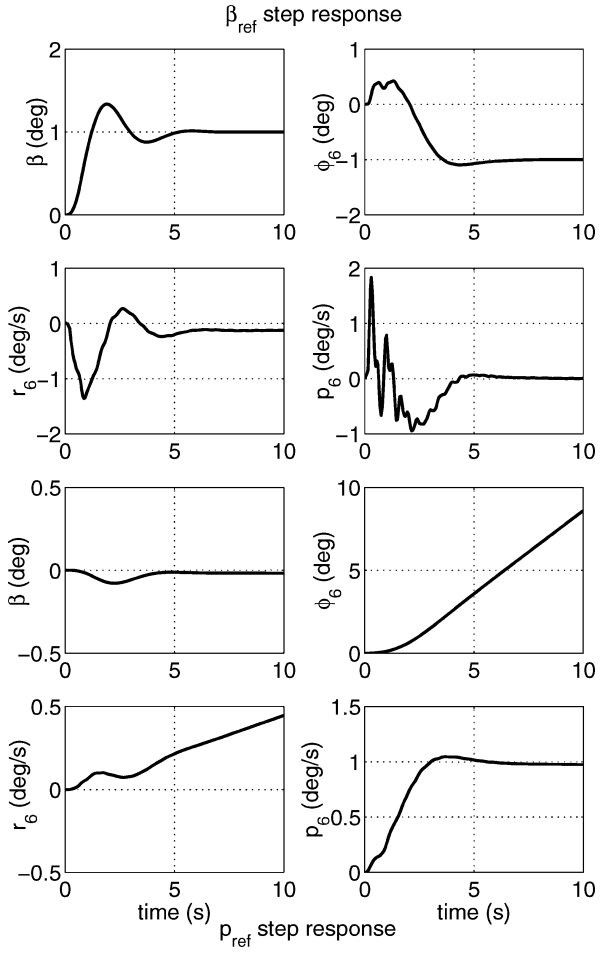

Fig. 15 Simulations: $K_{c_r}(1,4) = 2K_{c_r}(1,4)$.

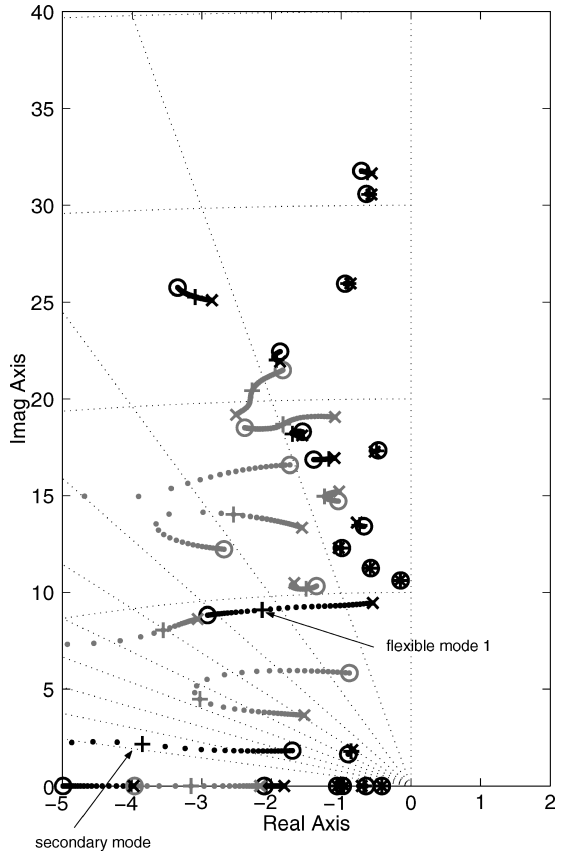

Fig. 16 Root locus around K_{c_1}.

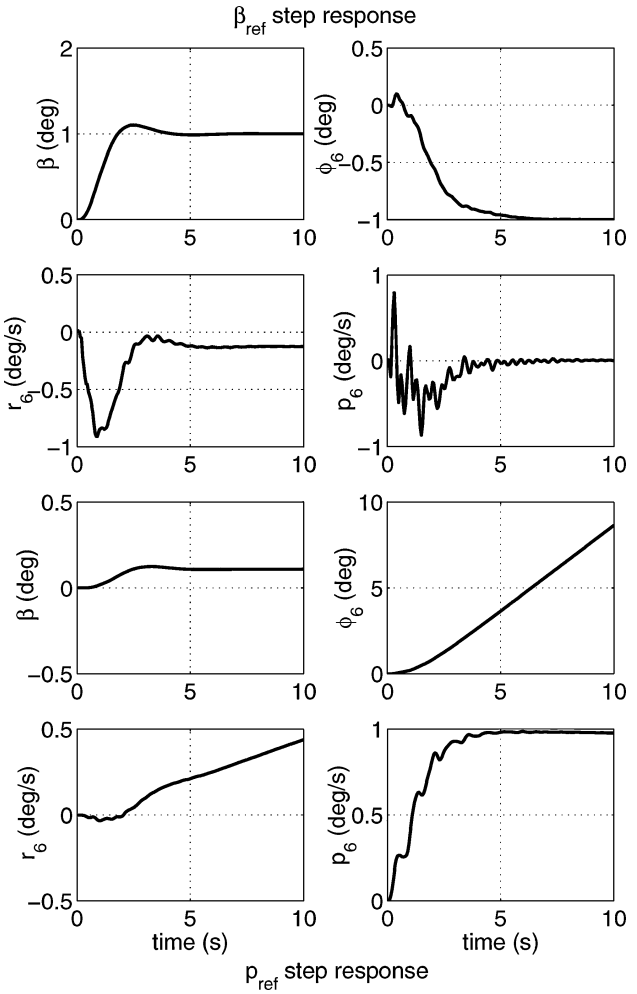

Fig. 17 Simulations: $K_{c_r} = K_{x_r}$.

adjustment. (Compare $G_{\Theta_0}^{-1}$ condition numbers.) However, this superior relevance is debatable because of the high value of the corresponding $G_{\Theta_0}^{-1}$: It highlights that all modes move more significantly in Fig. 12 than in Fig. 16.

Conclusions

The problem raised in this paper is twofold.

1) What kind of controller structure is of interest for postsynthesis tuning, that is, a structure where intuitive tuning directions can be easily highlighted?

2) Once these tuning directions are isolated, how can their efficiency be evaluated on the validation model?

When the controller order is greater or equal to the validation model order, the controller observer-based realization, involving the validation model, and the modal control theory allow tuning directions to be found to master any closed-loop eigenvalues assignment. When the controller order is lower than the validation model, the equivalent observer-based form, applied to a block-diagonal model of the main flexible and rigid behaviors, allows the initial controller to be implemented according to a parallel structure in which efficient tuning potentiometers can be isolated. Each potentiometer allows the effect of the control law on a specific mode associated with this potentiometer to be changed without major changes on the other modes.

The effectiveness of these potentiometers has been quantified by the parametric sensitivity analysis PRABI and has been verified by direct inspection of the time-domain response or flexible mode damping ratio and direct application of good sense rule. From a practical point of view, however, the main interest of such an approach is to perform in situ last-minute tuning in a flight test campaign, for instance.

Again note that tuning directions are here defined by intuitive considerations. To make this modal tuning method more general, further work will be focused on the tuning direction synthesis, that is, a theoretical obtention of the tuning directions. The PRABI, used here for the tuning direction analysis, could be exploited for this complementary step.

Acknowledgments

This work was carried out in collaboration with EADS/Airbus and with the support of Service Programme Aéronautique, Direction Générale de l'Armement.

References

[1]Balas, G., and Doyle, J., "Control of Lightly Damped, Flexible Modes in the Controller Crossover Region," *Journal of Guidance, Control, and Dynamics*, Vol. 17, No. 2, 1994, pp. 370–377.

[2]Tahk, M., and Speyer, J., "Parameter Robust Linear-Quadratic-Gaussian Design Synthesis with Flexible Structure Control Applications," *Journal of Guidance, Control, and Dynamics*, Vol. 12, No. 3, 1989, pp. 460–468.

[3]Alazard, M., Chrétien, J., and Du, M. L., "Attitude Control of a Telescope with Flexible Modes," *Dynamic and Control of Structures in Space*, Vol. 3, Computational Mechanics, London, 1996, pp. 167–184.

[4]Sato, M., and Suzuki, M., "Vibration Control of Flexible Structures Using a Combined $\mathcal{H}_\infty$ Filter Approach," *Journal of Guidance, Control, and Dynamics*, Vol. 19, No. 5, 1996, pp. 1000–1006.

[5]Joshi, S., and Kelkar, A. G., "Inner Loop Control of Supersonic Aircraft in the Presence of Aeroelastic Modes," *IEEE Transactions on Control Systems Technology*, Vol. 6, No. 6, 1998, pp. 730–739.

[6]Kubica, F., Livet, T., Le Tron, X., and Bucharles, A., "Parameter-Robust Flight Control System for a Flexible Aircraft," *Control Engineering Practice*, Vol. 3, No. 9, 1995, pp. 1209–1215.

[7]Zhou, K., "A New Controller Architecture for High Performance, Robust and Fault Tolerant Control," 39th Conference on Decision and Control, IEEE, Press, Piscataway, NJ, 2000, pp. 4120–4125.

[8]Alazard, D., and Apkarian, P., "Exact Observer-Based Structures for Arbitrary Compensators," *International Journal of Robust and Non-Linear Control*, Vol. 9, No. 2, 1999, pp. 101–118.

[9]Lavigne, G., "Dualité: qualité de l'identification—insensibilité de la commande. Application à la synthèse de commandes robustes aux incertitudes paramétriques," Ph.D. Dissertation, École Nationale Supérieure de l'Aéronautique et de l'Espace, Toulouse, France, Dec. 1994.

[10]Gauvrit, M., and Alazard, D., "Parametric Worst-Case Analysis by PRABI Method: Application to Flexible Space Structures," *2nd IFAC Symposium on Robust Control Design*, Cs. Bányácz, Budapest, Hungary, 1997, pp. 435–440.

[11]Cumer, C., "Techniques de Commande Robuste Approche Par Multiplicateurs et Approche Stochastique," Ph.D. Dissertation, École Nationale Supérieure de l'Aéronautique et de l'Espace, Toulouse, France, Dec. 1998.

[12]Alazard, D., "Robust H_2 Design for Lateral Flight Control of a Highly Flexible Aircraft," *Journal of Guidance, Control, and Dynamics*, Vol. 25, No. 3, 2002, pp. 502–509.

[13]Alazard, D., "Extracting Physical Tuning Potentiometers from a Complex Control Law: Application to Flexible Aircraft Flight Control," AIAA Paper 2001-4102, Aug. 2001.

[14]Magni, J., Gorrec, Y. L., and Chiappa, C., "A Multimodel-Based Approach to Robust and Self-Scheduled Control Design," *Proceedings of the 37th IEEE Conference on Decision and Control*, IEEE Press, Piscataway, NJ, 1998, pp. 3009–3014.

[15]Magni, J., *Robust Modal Control with a Toolbox for Use with Matlab®*, Kluwer Academic/Plenum, New York, 2002.

[16]Champetier, C., and Magni, J., "Analysis and Synthesis of Modal Control Laws," *Recherche Aérospatiale*, Vol. 6, 1989, pp. 17–35.

[17]Tischler, M. B., *Advances in Aircraft Flight Control*, Taylor and Francis, Philadelphia, 1996.